DEUTSCHES ELEKTRONEN-SYNCHROTRON DESY

DESY SR-79/07
March 1979

TIME AND SPECTRALLY RESOLVED FLUORESCENCE OF Xe_2 MOLECULES EXCITED WITH SYNCHROTRON RADIATION

by

H. D. Wenck, S. S. Hasnain, M. M. Nikitin

K. Sommer, G. Zimmerer

II. Institut für Experimentalphysik der Universität Hamburg
and
Deutsches Elektronen-Synchrotron DESY, Hamburg

D. Haaks

Institut für Physikalische Chemie der Gesamthochschule Wuppertal

NOTKESTRASSE 85 · 2 HAMBURG 52

To be sure that your preprints are promptly included in the
HIGH ENERGY PHYSICS INDEX ,
send them to the following address (if possible by air mail) :

DESY
Bibliothek
Notkestrasse 85
2 Hamburg 52
Germany

TIME AND SPECTRALLY RESOLVED FLUORESCENCE OF Xe_2 MOLECULES EXCITED WITH SYNCHROTRON RADIATION

H.D. Wenck, S.S. Hasnain*, M.M. Nikitin**,

K. Sommer, G. Zimmerer.

II. Institut für Experimentalphysik der Universität Hamburg,

D-2000 Hamburg 50, Germany,

and Deutsches Elektronen-Synchrotron DESY, d-2000 Hamburg 52, Germany,

and

D. Haaks,

Institut für Physikalische Chemie der Gesamthochschule Wuppertal,

D-5600 Wuppertal 1, Germany.

* Present address: Departments of Chemistry and Medical Biophysics, University of Manchester, England.

** On leave from Scientific Research Institute of Nuclear Physics, Tomsk Polytechnic Institute, Tomsk, U.S.S.R.

ABSTRACT

Time and energy resolved fluorescence of Xe has been investigated using pulsed synchrotron radiation. The radiative lifetime of the relaxed Xe_2^* (1_u) and its collisional mixing with Xe_2^* (0_u^+) are measured. Rate constants for molecule formation are deduced. Different steps of the reaction kinetics are isolated by using various excitation wavelengths.

1. Introduction

Diatomic rare gas molecules like Xe_2^* are prototypes for the variety of excimers with their outstanding properties for laser application (1). Fluorescence spectroscopy is an important tool to investigate the creation of excimers as well as their electronic states. The excimeric fluorescence of Xe_2^* consists of the well known 1st ($\sim$ 1520Å) and 2nd ($\sim$ 1700Å) continuum. Radiative transition from vibrationally excited 0_u^+ state to the ground state 0_g^+ is responsible for the first continuum while the 2nd continuum results from the vibrationally relaxed 0_u^+ and 1_u state. Details of the fluorescence spectra sensitively depend on the gas pressure and on the excitation energy (2).

Here we report results from a time-and spectrally resolved fluorescence study of gaseous Xe. The gas is excited with monochromatic VUV light in the vicinity of the first resonance line ($1470Å, {}^1S_o \rightarrow {}^3P_1$) of Xe. In order to understand various relaxation processes, comprehensive measurements were made by scanning the excitation wavelength from the blue wing to the red wing of the first resonance line with steps of 10 Å (1450 Å - 1550 Å). The first continuum decay functions were measured for gas pressures between 50-500 torr and the second continuum was investigated between 250 and 1050 torr. The measurements yield information about the life-time of the relaxed 1_u states and its collisional mixing with the 0_u^+ state. Molecular formation takes place via three-body collision. Rate constants for the molecule formation are deduced. The results are of particular interest as controversial results have been recently published (3-5).

2. Experiment

For excitation the synchrotron radiation of the electron storage ring DORIS at Hamburg was used. Synchrotron radiation was monochromated with a band pass of 3 Å and then focussed into a LiF gas cell. The illuminated part of the cell serves as an entrance slit for a VUV monochromator for the spectral analysis of fluorescence (band pass 30Å). Time resolution is obtained by making use of the pulse structure of the synchrotron radiation of DORIS (fwhm of light pulses is 130 ps, repetition rate is 1 MHz). The experimental techniques are described in detail in ref (6). Fast photomultiplier (BX 762) was used with a time resolution of $\sim$ 2 ns. Although very fast procecces ($k > 10^8\ S^{-1}$) were established we restrict ourselves to "slow" decay rates $k < 5 \cdot 10^7\ S^{-1}$ ($\hat{=}\ \tau = 1/k > 20ns$).

3. Results and Evaluation of the Data

In Fig. 1 typical decay curves of the 1st continuum are shown. Fig. 2 shows the time resolved spectra of the 2nd continuum under red wing excitation (λ_{exc} = 1490Å and 1500Å, Fig. 2a) and λ_{exc} = 1470Å excitation (Fig. 2b). In both continua, very fast processes (decay rates $k_{fast} > 10^8\ S^{-1}$) coexist with slower processes ($k_i < 5 \cdot 10^7\ S^{-1}$).

The slow contribution to the 1st continuum is dominated by one single exponential (decay rate $k^{(1)}$). k_{fast} dominates more as we excite further into the red wing (i.e. $\lambda > 1490Å$). For a fixed wavelength in the red wing a similar trend holds for decreasing pressure.

In the second continuum, k_{fast} is generally weak. For $\lambda_{exc} > 1470\text{Å}$ it is always present but for $\lambda_{exc} \leq 1470\text{Å}$ it can hardly be detected. The slow part of the 2nd continuum includes very pronounced rise times and can no longer be described by a single exponential. Therefore, the time resolved spectra were fitted by a sum of exponentials (least sqare fits). Only those parts of the spectra were used in which the components k_{fast} have already disappeared.

The decay rates, $k_i^{(2)}$, of the 2nd continuum are displayed in Fig. 3. For excitation far into the red wing ($\lambda_{exc} > 1500\text{Å}$) only one rate, $k_1^{(2)}$ is found, (Fig. 3a). For excitation in the near red wing ($1500\text{Å} > \lambda_{exc} > 1470\text{Å}$) an additional decay rate $k_2^{(2)}$ is seen. A third rate, $k_3^{(2)}$ can be identified in a limited pressure range (Fig. 3c) for resonant $Xe^* {}^3P_1$ and blue wing excitation ($\lambda_{exc} \leq 1470\text{Å}$).

The necessity for introducing a third rate arose because the standard deviation for a fit with only two exponentials (like in Fig. 3a,3b) was drastically worse for $\lambda_{ex} \leq 1470\text{Å}$ than for $\lambda_{ex} > 1470\text{Å}$. In general a fit of decay curves including three exponentials does not give well defined values for the fitting parameters. We reduced the number of adjustable exponentials to two assuming the same pressure dependence of $k_1^{(2)}$ in Fig. 3c as in Fig. 3a and Fig. 3b.

The full line for $k_1^{(2)}$ in Fig. 3 is a least sqare fit which yields a pressure dependence $k_1^{(2)} = k_{1,0}^{(2)} + \alpha_1 p$ with $k_{1,0}^{(2)} = 9.9 \cdot 10^6\ s^{-1}$ $\hat{=}$ 101 ns and $\alpha_1 = 3{,}1 \cdot 10^{-14}\ cm^3\ s^{-1}$. The pressure dependence of $k_2^{(2)}$ can be fitted as $k_2^{(2)} = \alpha_2 p + \beta_2 p^2$ with $\alpha_2 = 7.8 \cdot 10^{-14}\ cm^3\ s^{-1}$ and $\beta_2 = 7.5 \cdot 10^{-32}\ cm^6\ s^{-1}$. Within the experimental scatter, the points

of $k^{(1)}$ fit the same expression.

The scatter of the few points of $k_3^{(2)}$ does not enable a safe analysis. Assuming $k_3^{(2)} = \alpha_3 p + \beta_3 p^2$ one obtains $\alpha_3 = 1{,}1 \cdot 10^{-12}$ $cm^3\ s^{-1}$ and $\beta_3 = 5.2 \cdot 10^{-32}\ cm^6\ s^{-1}$. A simple p^2 fit yields $\beta_3 = 1{,}6 \cdot 10^{-31}\ cm^6\ s^{-1}$.

4. Discussion of the results

In order to facilitate the discussion, potential curves of Xe_2 are given in Fig. 4. We first consider the results for red-wing excitation $\lambda_{exc} > 1470\text{Å}$ for the first continuum.

In this case, the formation and the radiative decay of Xe_2^* is described by:

$$Xe_2(0_g^+) + h\nu \rightleftarrows Xe_2^* \ (0_u^+(v)) \qquad (1)$$

In addition to the direct radiative decay, vibrational relaxation takes place with a two-body rate constant of $8 \cdot 10^{-11}\ cm^3\ s^{-1}$ (7). This together with intersystem crossing leads to the population of the states showing up in the 2nd continuum (see below). The long decay rate in the 1st continuum can only be understood if the population of a metastable reservoir takes place on the time scale of k_{fast} through an additional decay channel. This channel may be collision assisted. Molecules may be dissociated into the metastable $Xe^* {}^3P_2$ or even into the radiation trapped $Xe^* {}^3P_1$. Please, note the crossing of the 0_u^+ state with dissociative states terminating at $^3P_2$ (Fig. 4). The relative amount of $Xe^* {}^3P_2$ and $Xe^* {}^3P_1$ may be a sensitive function of excitation wavelength.

The metastable reservoir then feeds back into the 1st continuum via three body collision:

$$Xe^* + 2Xe \xrightarrow{k^{(1)}} Xe_2^* (0_u^+(v)) + Xe \qquad (2)$$

The slow decay of the 1st continuum can directly be related to the molecule formation $k^{(1)}$ because the effective lifetime of vibrationally excited Xe_2^* molecules is always very small compared to the rate of molecule formation for the pressure range under investigation. The fact that the relative intensity of the long component decreases with decreasing pressure supports our assumption of a collision assisted population of the metastable reservoir. The decrease of the relative intensity of the long component with decreasing excitation energy is due to the increasing energetic difference between the initially excited state and the energy of the reservoir.

For $\lambda_{exc} \geq 1500\text{Å}$, the long component in the 1st continuum and consequently the population of the metastable reservoir is negligible. The $v = o$ 0_u^+ and 1_u states which show up in the 2nd continuum are populated via vibrational relaxation and intersystem crossing. The decay of 0_u^+ is responsible for the fast component in the 2nd continuum. $k_1^{(2)}$ describes the decay of 1_u states. The linear pressure dependence of $k_1^{(2)}$ (see Fig. 3a) is attributed to collisional mixing of 1_u and 0_u^+ states with two body rate constant of $3,1 \times 10^{-14}$ $cm^3\ s^{-1}$. The value of $k_1^{(2)}$ obtained by extrapolation to zero pressure yields a radiative lifetime of 101 ns for the relaxed 1_u state.

For $1470\text{Å} < \lambda_{exc} < 1490\text{Å}$ population of the metastable reservoir after initial excitation cannot be neglected. In that case the 2nd continuum states are populated via (a) relaxation immediately after the creation of Xe_2^* molecules (see above) and, (b) creation of molecules starting from the metastable reservoir, followed by relaxation. The p^2-contribution of $k_2^{(2)}$ is attributed to molecule formation and is the same process as is seen in the 1st continuum. In the second continuum the

rate of formation of the molecules and the decay rate of the 1_u state clearly cross at a pressure of $\sim$ 350 torr (Fig. 3b).

The origin of the weak linear contribution to $k_2^{(2)}$ is not clear. The measured rate constant may be a superposition of loss processes in the metastable reservoir like collision induced transitions, energy transfer to traces of impurities and collisional mixing between $^3P_1$ and $^3P_2$.

Under resonant excitation of Xe^* ($^3P_1$) (1470Å) both Xe^* ($^3P_1$) atoms and Xe_2^* molecules are produced due to the band pass of the exciting light. The molecule is formed in the repulsive 1_u state or the bound 0_u^+ state both terminating at the $^3P_1$ level. Excitation with $\lambda_{exc} < 1470\text{Å}$ leads to the repulsive 1_u state. Compared to red wing excitation, a great part ($\lambda_{exc} = 1470\text{Å}$) or even all the excitation energy is immediately stored in the metastable reservoir and consequently the long components dominate in both continua. Nevertheless, in the 1st continuum, the directly excited 0_u^+ molecules manifest themselves in the still existing fast component which, however, can no longer be deduced in the 2nd continuum with confidence.

The existence of two decay rates with a p^2-contribution, $k_2^{(2)}$ and $k_3^{(2)}$, in the 2nd continuum under resonant and blue wing excitation can be tentatively assigned to molecule formation starting from either Xe^* ($^3P_2$) or Xe^* ($^3P_1$) atoms. It is plausible that $k_3^{(2)}$ is only measurable under resonant or blue wing excitation. Then the 2nd continuum is exclusively populated via the metastable reservoir. Under red wing excitation, a great fraction of the 2nd continuum is populated directly via relaxation of the initially excited molecular states. The fraction which includes the metastable reservoir is obviously not large enough to bring $k_3^{(2)}$ into play as well under the red wing excitation. Moreover, under red wing

excitation the fast component, k_{fast}, does not allow for a safe fit of the rising part of the time resolved spectra. The values of $k_3^{(2)}$ are more sensitive to the rising part than to the decay.

5. Comparison with literature values

Our numerical results are summarised in table 1. The result for the radiative lifetime of the relaxed $^1\Sigma_u$ state agrees well with the values reported in Refs (7-11). The value reported by Ghelfenstein et al (3) (60 ns) can be ruled out. The decay times of the 2nd continuum measured by O. Dutuit et al (4) fit into our curve of $k_2^{(2)}$ extrapolated to low pressures. We cannot follow the conclusion of Poliakoff et al who discuss their result of 112 ns as a lower limit for the radiative lifetime of the relaxed $^1\Sigma_u$ state (5).

The result for the collisional mixing of $^1\Sigma_u$ and 0_u^+ (upward reaction) is in qualitative agreement with (7, 12). Good agreement with other measurements is found for the threebody rate constant deduced from $k_2^{(2)}$. The rate constant tentatively deduced from $k_3^{(2)}$, to our knowledge, up to now has not been measured before.

The general agreement with rerent experiments using either e- (9,10,12) or α-particle excitation (11) demonstrates that monochromatic synchrotron radiation is a powerful tool for sorting our various competing relaxation processes and reaction kinetics. It enables an even more detailed analysis than data obtained with unspecific excitation. Finally, with present data we clarify the situation of controversial results obtained in earlier experiments with synchrotron radiation.

Acknowledgements

We thank Drs. M.C. Castex and J. Le Calvé for valuable discussions and Drs. U. Hahn and N. Schwentner for experimental support. Thanks are due to the Bundesministerium für Forschung und Technologie BMFT for financial support. S.S.H. thanks DESY for granting a visiting fellowship.

References

(1) C.W. Werner, E.V. George, P.W. Hoff, and C.K. Rhodes, IEEE J. Quantum Electronics QE-13, 769 (1977)

(2) R. Brodmann and G. Zimmerer, J. Phys. B.: Atom. Molec. Phys. 10, 3395 (1977)

(3) M. Ghelfenstein, R. Lopez-Delgado, and H.S. Szware, Chem. Phys. Letters 49, 312 (1977)

(4) O. Dutuit, R.A. Gutchek, and J. Le Calvé, Chem. Phys. Letters 58, 66 (1978)

(5) E.D. Poliakoff, M.G. White, R.A. Rosenberg, G. Thornton, E. Matthias, and D.A. Shirley, LBL-7651 Preprint, to be published in J. Chem Phys.

(6) U. Hahn, N. Schwentner, and G. Zimmerer, Nuclear Instr. and Methods 152, 261 (1978)

(7) T.D. Bonifield, F.H.K. Rambow, G.K. Walters, M.V. McCusker, D.C. Lorents, and R.A. Gutchek, Stanford Synchrotron Radiation Laboratory SSRL Report No. 9 (1978), p. 85

(8) D. Haaks, to be published

(9) J.W. Keto, R.E. Gleason, Jr., and G.K. Walters, Phys. Rev. Letters 33, 1365 (1974

(10) P.K. Leichner, K.F. Palmer, J.D. Cook, and M. Thienemann, Phys. Rev. A13, 1787 (1976)

(11) P. Millet, A. Birot, H. Brunet, J. Galy, B. Pons-Germain, and J.L. Teyssier, J. Chem. Phys. 69, 92 (1978)

(12) J.W. Keto, R.E. Gleason, Jr., T.D. Bonifield, G.K. Walters, and F.K. Soley, Chem. Phys. Letters 42, 125 (1976)

(13) P.R. Timpson and J.M. Anderson, Can. J. of Physics 48, 1817 (1970)

(14) M.C. Castex, private communication

(15) W.C. Ermler, Y.S. Lee, K.S. Pitzer and N.W. Winter, J. Chem. Phys. 69, 976 (1978)

- - - - -

TABLE 1

Three-body rate constants and lifetimes obtained from our measurements with synchrotron radiation and comparison with some literature values (compilation not complete).

this paper	literature values	excitation source
radiative lifetime of the relaxed Xe_2^* (1_u) state in ns		
(101 ± 1)	(96±5) (9); 99(10); (100+2) (12) (102+2) (11) (101±20) (8)	e^--beam α - particles discharge lamp
	60 (3); 112 (5); 100 (7)	synchrotron radiation
rate constant for Xe_2^* (1_u) ⟶ Xe_2^* (0_u^+) in $cm^3\ s^{-1}$		
$3.1 \cdot 10^{-14}$	$(6.6 \pm 1.8) \cdot 10^{-15}$ (12) $4.6 \cdot 10^{-15}$ (7)	e^--beam synchrotron radiation
rate constant for Xe + 2Xe ⟶ Xe_2 + Xe in $cm^6 s^{-1}$		
$7.8 \cdot 10^{-32}$	$8 \cdot 10^{-32}$(13); $(8\pm0.7)\cdot10^{-32}$ $4 \cdot 10^{-32}$(10); $7.8 \cdot 10^{-32}$(8)	afterglow (13) other Refs. see above
$5.2 \cdot 10^{-32}$ or $1.6 \cdot 10^{-31}$	?	

Figure Captions

Fig. 1 Decay curves of the 1st continuum measured at 1520Å. For each curve the pressure (in torr) and the excitation wavelength (in Å) is given in the figure. Intensity is plotted in a logarithmic scale. The time scale is the same for all curves. The zero point is shifted from curve to curve

Fig. 2 Decay curves of the 2nd continuum measured at 1700Å. a) red wing excitation, b) resonant excitation (1470Å). The pressures are given in the figure.

Fig. 3 Decay rates $k_1^{(2)}$, $k_2^{(2)}$, $k_3^{(2)}$ of the 2nd continuum as a function of gas pressure for different excitation wavelengths (given in the figure).

Fig. 4 Potential curves of Xe_2, based on a recent careful analysis of experimental data (14) and theoretical calculations (15). Repulsive $^2{}_{g,u}$ states terminating at $^3P_2$ are omitted.

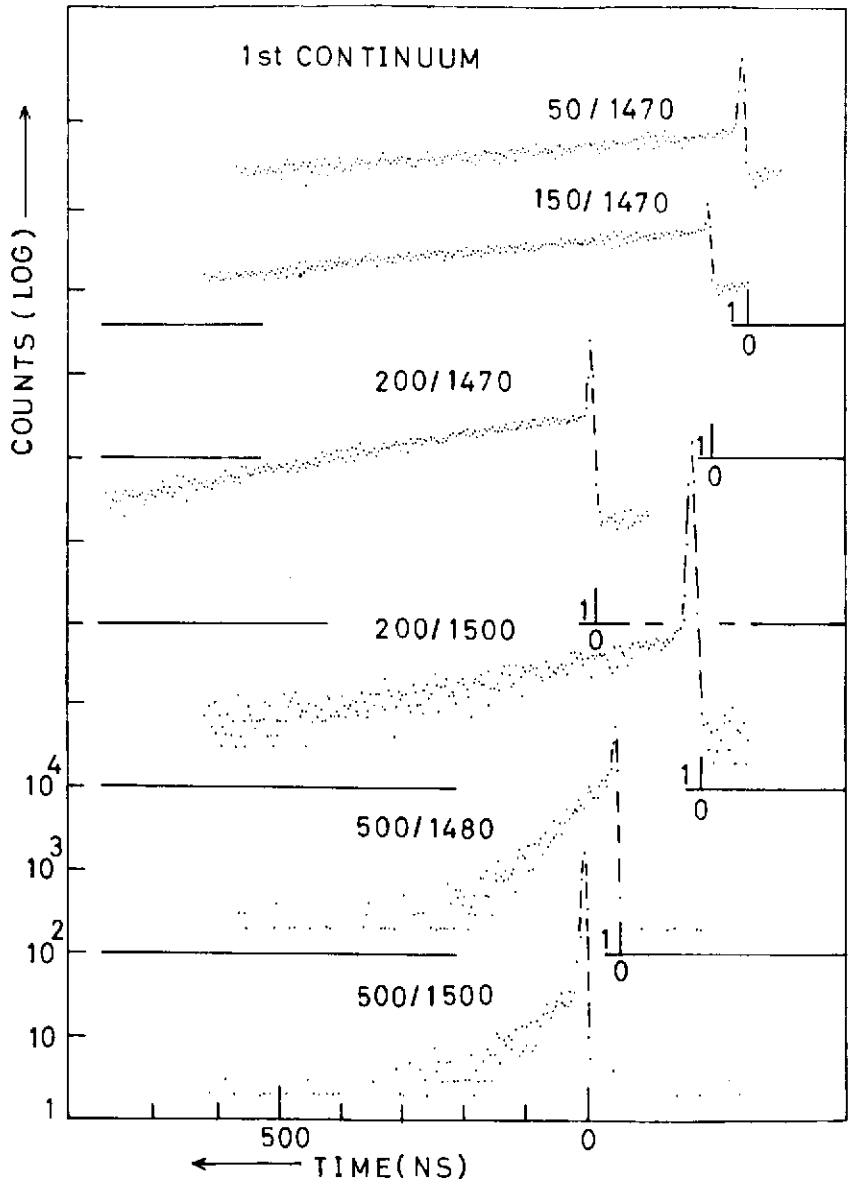
1st CONTINUUM
50 / 1470
150/ 1470
200/1470
200/1500
500/1480
500/1500
COUNTS (LOG)
TIME(NS)
500
0
1
10
10^2
10^3
10^4

Fig. 1

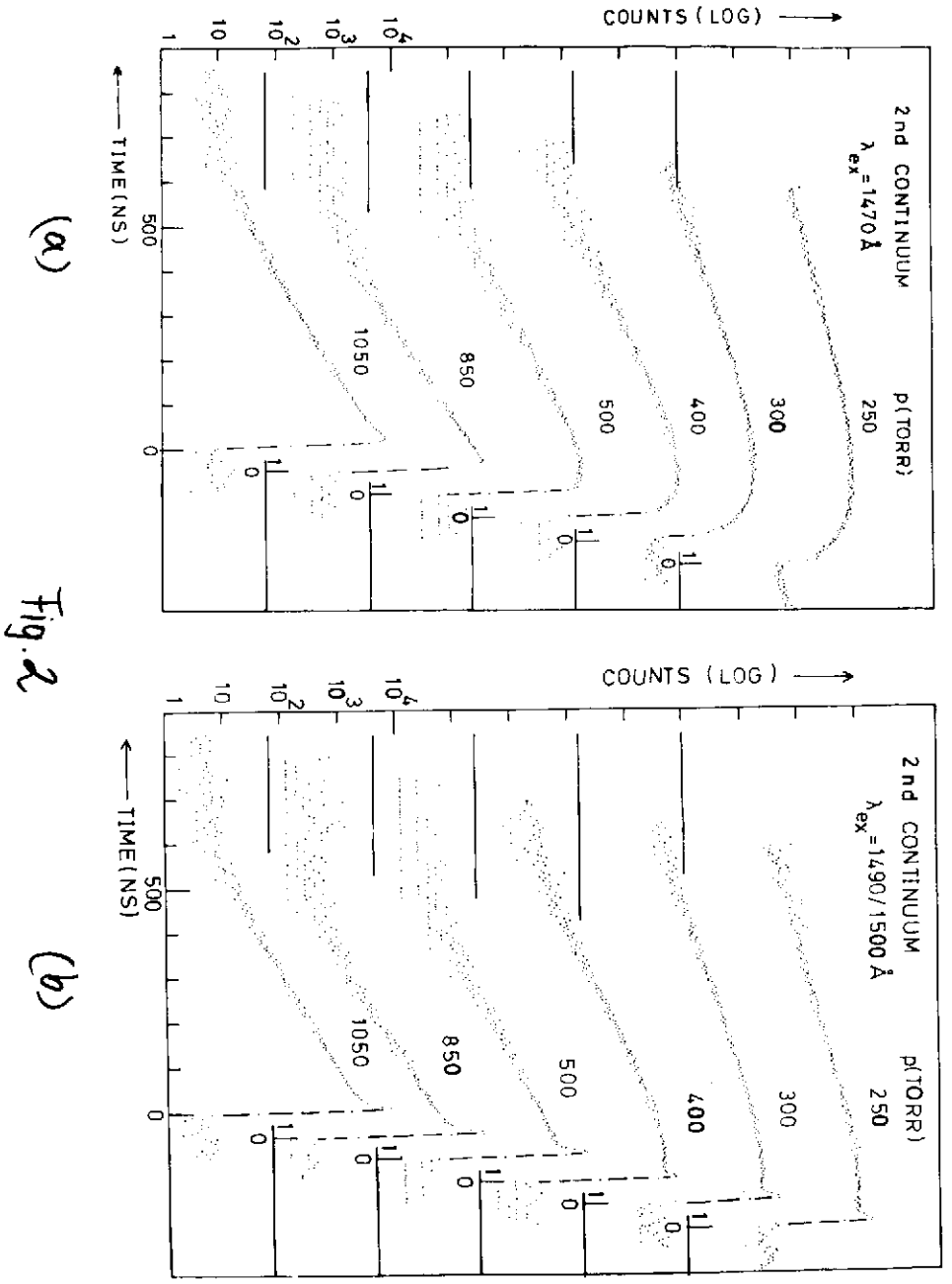
(a)
(b)
COUNTS (LOG)
TIME(NS)
2nd CONTINUUM
λex=1470 Å
λex=1490/1500 Å
p(TORR)
1050
850
500
400
300
250
500
0
1
10
10^2
10^3
10^4

Fig. 2

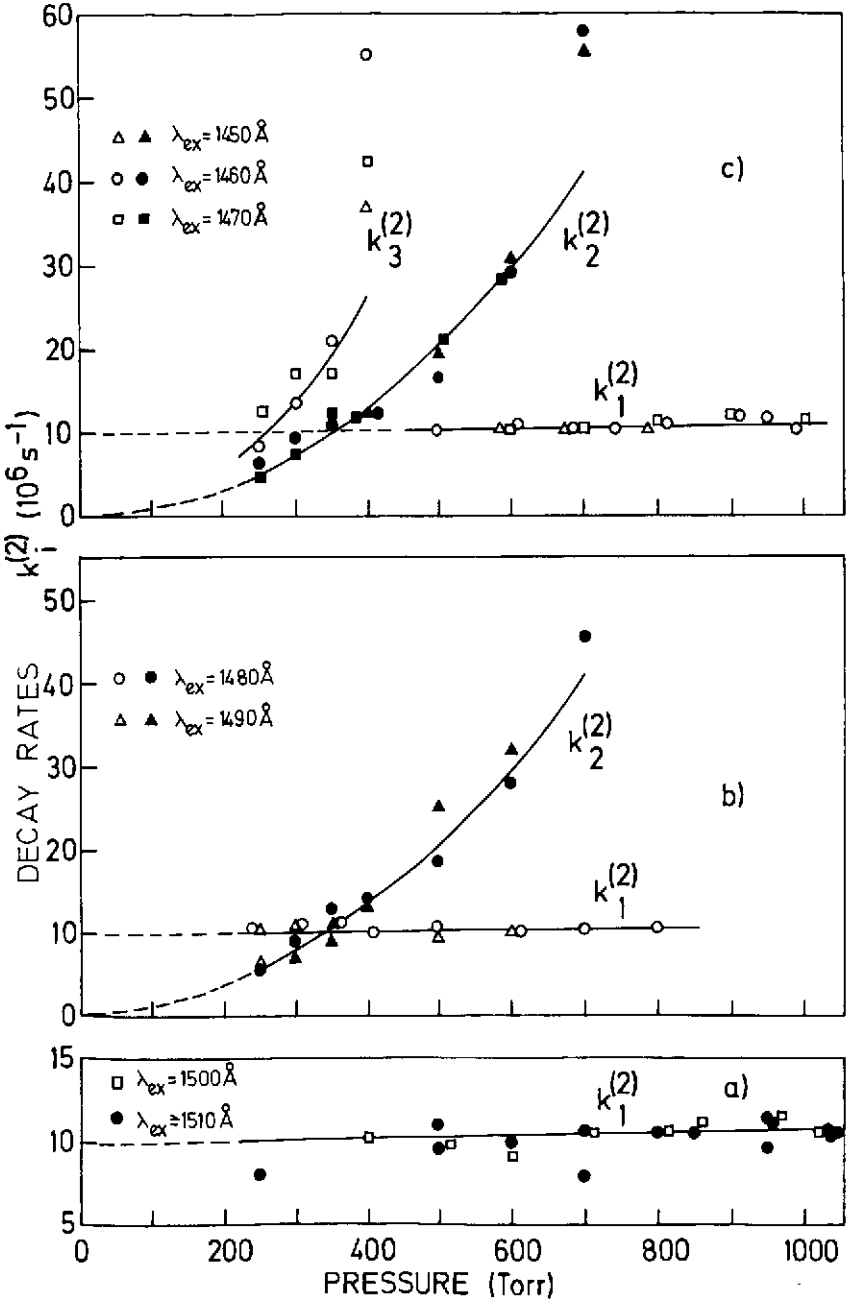
DECAY RATES $k_i^{(2)}$ $(10^6 s^{-1})$
λ_{ex} = 1450 Å
λ_{ex} = 1460 Å
λ_{ex} = 1470 Å
c)
$k_3^{(2)}$
$k_2^{(2)}$
$k_1^{(2)}$
λ_{ex} = 1480 Å
λ_{ex} = 1490 Å
b)
λ_{ex} = 1500 Å
λ_{ex} = 1510 Å
a)
PRESSURE (Torr)

Fig. 3

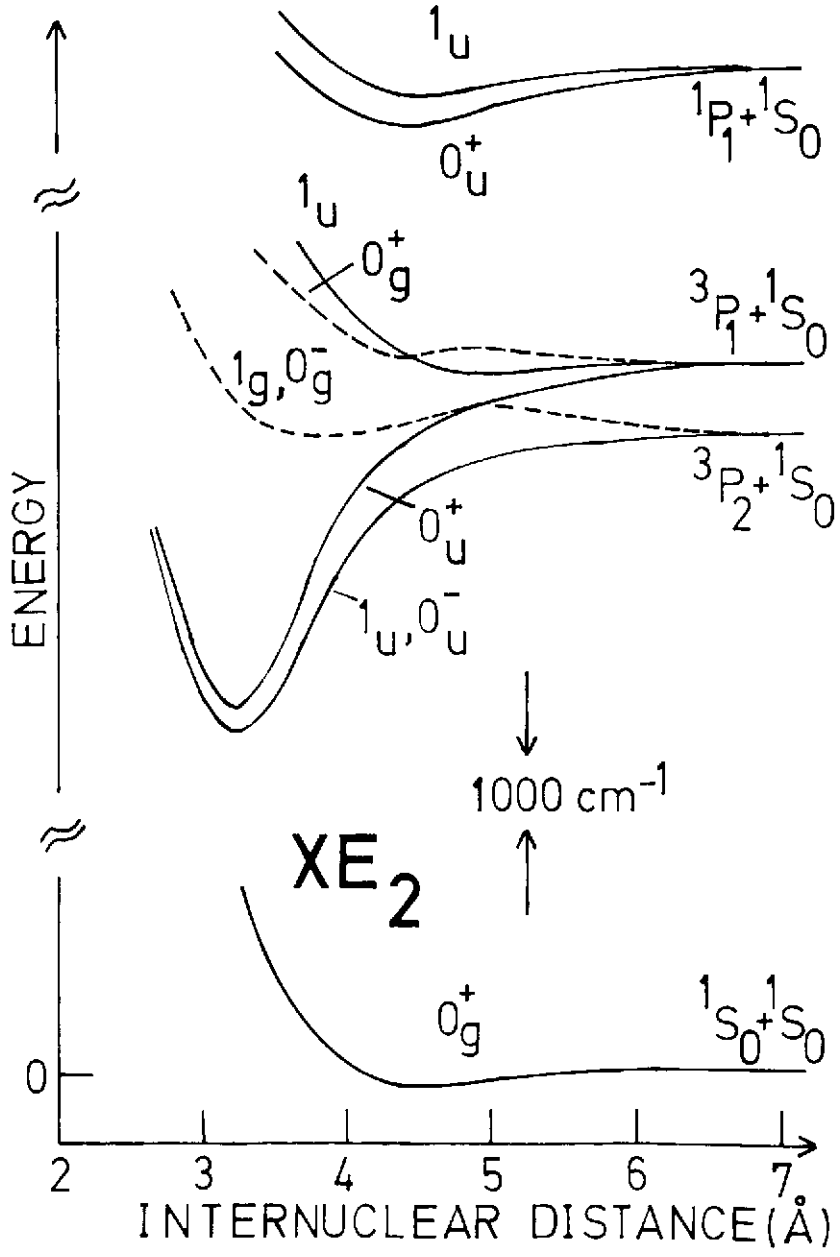
ENERGY
^1u
0_u^+
$^1P_1 + {}^1S_0$
^1u
0_g^+
$^3P_1 + {}^1S_0$
$^1g, 0_g^-$
$^3P_2 + {}^1S_0$
0_u^+
$^1u, 0_u^-$
1000 cm^{-1}
XE_2
0_g^+
$^1S_0 + {}^1S_0$
0
2
3
4
5
6
7
INTERNUCLEAR DISTANCE (Å)

Fig. 4